J|A|C|S
ARTICLES
Published on Web 11/16/2002

Exploring Nucleoside Hydrolase Catalysis *in Silico*: Molecular Dynamics Study of Enzyme-Bound Substrate and Transition State

Devleena Mazumder and Thomas C. Bruice*

Contribution from the Department of Chemistry and Biochemistry, University of California, Santa Barbara, Santa Barbara, California 93106

Received August 15, 2002

Abstract: The mechanism of action of inosine-uridine nucleoside hydrolase has been investigated by long-term molecular dynamics (MD) simulation in TIP3P water using stochastic boundary conditions. Five MD studies have been performed with enzyme substrate complex (E·S), enzyme substrate complex with protonated His241 (EH·S), enzyme transition state complex (E·TS), enzyme transition state complex with protonated His241 (EH·TS), and His241Ala transition state complex E(H241A)·TS. Special attention has been given to the role of His241, which has been considered as the general acid catalyst to assist departure of the leaving nucleobase on the basis of its location in the active site in the X-ray crystal structure (2MAS). Yet on the basis of the location in the active site, Tyr229 is closer to the aniline ring of pAPIR as compared to His241. On initiation of MD simulations, His241 does not approach the nucleobase in the structures of EH·S, E·S, EH·TS, and E·TS. In the solvated enzyme, Tyr229, which is a member of the hydrogen bonding network inosine O2'··Asp14··His241··Tyr229··inosine N7, serves as a proton source to the leaving nucleobase. The loss of significant activity of His241Ala mutant is shown to be related to the disruption of the above hydrogen bonded network and the distancing of Tyr229 from inosine N7. The structures of the enzyme complexes with substrate or TS are not visibly altered on protonation of His241, a most unusual outcome. The bell-shaped pH dependence upon pK_{app}'s of 7.1 and 9.1 may be attributed to the necessity of the dissociation of Asp10 or Asp15 and the acid form of Tyr229, respectively. In TS, the residue Ile81 migrated closer, whereas Arg233 moved away from the nucleobase. The probability of ribooxocarbenium ion stabilization by Asn168 and Asp14 is discussed. The Asp14-CO_2^- is hydrogen bonded to the ribose 2'-OH for 96% of the MD simulation time. Nucleophilic addition of water138 to ribooxocarbenium ion is suggested to be assisted by the proton shuttle from water138 → Asp10 → Asp15 → water pool. An anticorrelation motion between Tyr229-OH and Asn168-OD1 in EH·S and E·S is observed. The relationship of this anticorrelated motion to mechanism, if any, deserves further exploration, perhaps the formation of a near attack conformation.

Introduction

Parasitic diseases are a major threat to human and animal health across the global rural population. The protozoan parasites lack a *de novo* biosynthetic pathway for purines and rely exclusively on purine salvage from the host nucleosides.[1] The enzymatic hydrolysis of the *N*-ribosidic bond is a critical step in the purine salvage pathway. There is a great deal of interest in designing and developing inhibitors of protozoan nucleoside hydrolase as potential chemotherapeutic agents because no nucleoside hydrolase activity or genes encoding this enzyme have been identified in mammals.[2]

The inosine-uridine nucleoside hydrolase (IU-NH) from *Crithidia fasciculata* is a homotetramer of M_r 34 000 subunits.[3] Experimental techniques such as crystallography,[3,4] kinetic analysis,[5] and mutagenesis[2] have been used to understand the catalytic mechanism and the mode of binding as well as the favored protonation state[6] of the transition state analogue inhibitor *p*-aminophenyl-(1*S*)-iminoribitol or pAPIR. A basic interpolation of the profiles of V_{max}/K_M versus pH shows an unprotonated group with a pK_{app} of 7.1 and a protonated group with a pK_{app} of 9.1 required for catalysis but not for the binding of substrate.[5] Schramm and co-workers have offered the mechanism shown in Scheme 1.[7] The enzyme-catalyzed reaction follows an S_N1-like mechanism and proceeds via the ribooxocarbenium ion transition state.[7] It is proposed that an active site general base abstracts a proton from the incoming water to facilitate the nucleophilic attack at the C1′ of the ribose ring,

* To whom correspondence should be addressed. Phone: 805-893-2044. Fax: 805-893-2229. E-mail: tcbruice@bioorganic.ucsb.edu.

(1) Hammon, D. J.; Gutteridge, W. E. *Mol. Biochem. Parasitol.* **1984**, *13*, 243.
(2) Gopaul, D. N.; Meyer, S. L.; Degano, M.; Sacchettini, J. C.; Schramm, V. L. *Biochemistry* **1996**, *35*, 5963.
(3) Degano, M.; Gopaul, D. N.; Scapin, G.; Schramm, V. L.; Sacchettini, J. C. *Biochemistry* **1996**, *35*, 5971.
(4) Degano, M.; Almo, S. C.; Sacchettini, J. C.; Schramm, V. L. *Biochemistry* **1998**, *37*, 6277.
(5) Parkin, D. W.; Schramm, V. L. *Biochemistry* **1995**, *34*, 13961.
(6) Mazumder, D.; Kahn, K.; Bruice, T. C. *J. Am. Chem. Soc.* **2002**, *124*, 8825.
(7) Horenstein, B. A.; Parkin, D. W.; Estupiñán, B.; Schramm, V. L. *Biochemistry* **1991**, *30*, 10788.

Scheme 1

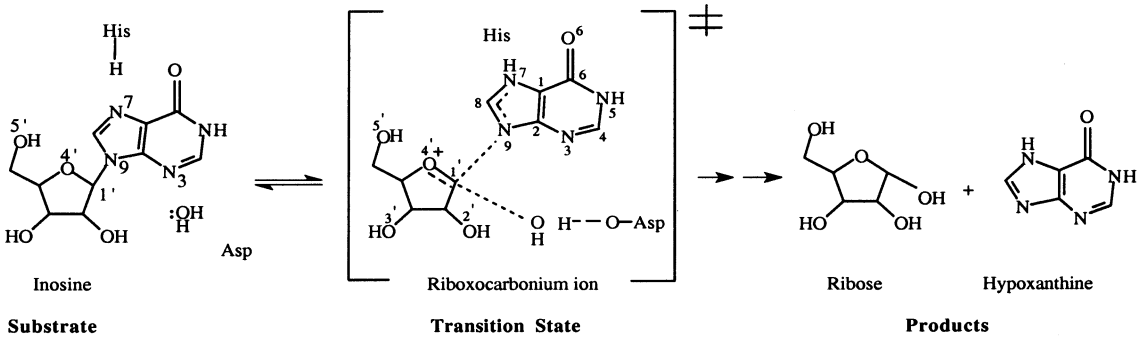

and an enzymatic general acid activates the purine leaving group. The protonation of N7 of the purine ring before reaching the transition state is proposed to lower the electron density in the purine ring, hence facilitating its departure. Three-dimensional structures of the free and the pAPIR inhibitor-bound IU-NH from *Crithidia fasciculata* (PDB ID: 1MAS,[3] 2MAS[4]) have been determined recently by X-ray crystallography. These X-ray structures have pointed out various enzymatic residues that interact with the ribose part of purine substrates and may stabilize the ribooxocarbenium ion transition state. The information about the interactions between the leaving group pocket and the natural substrates is difficult to extract from the currently available crystal structures of inhibitor bound IU-NH due to significant structural differences between the inhibitor and a purine/pyrimidine nucleoside, particularly in the base moiety.[8] Assumption of His241 as a general acid with an apparent pK_{app} of 9.1 was based on its location in the active site (pAPIR aniline ring nitrogen is 6.8 Å from the NE2 of His241 in the X-ray structure 2MAS) and mutagenesis results (mutation of His241Ala caused a 2100-fold loss in k_{cat} and an elevation in K_m by a factor of 3.5-fold).[2] The mutant enzyme had a residual activity of 10^{-3}.

Here, we report long-term molecular dynamics (MD) simulations of the following enzyme complexes: (i) enzyme·substrate with protonated His241 (EH·S), (ii) enzyme·substrate with neutral His241 (E·S), (iii) enzyme·transition state with protonated His241 (EH·TS), and (iv) enzyme·transition state with neutral His241 (E·TS). A short-term (600 ps) MD simulation of the enzyme·transition state complex using the mutant enzyme (H241A) was also carried out. From hereon, this MD simulation will be referred as E(H241A)·TS.

Methods

General Setup. Stochastic boundary molecular dynamics[9] were performed on nucleoside hydrolase using initial coordinates of IU-NH bound with a transition state analogue inhibitor pAPIR (Protein Data Bank code 2MAS[4]). On the basis of the knowledge of binding of the transition state analogue inhibitor from the X-ray crystallography, ground-state inosine and the transition state were docked to the IU-NH active site. Long-term molecular dynamics were performed on the following systems: enzyme·substrate with protonated His241, enzyme·substrate with neutral His241, enzyme·transition state with protonated His241, and enzyme·transition state with neutral His241. From hereon, these complexes will be referred as EH·S, E·S, EH·TS, and E·TS, respectively. A MD simulation on the mutant His241Ala enzyme complexed with TS was also performed. The starting coordinates of ground-state inosine were developed using Quanta. The partial structure

Chart 1

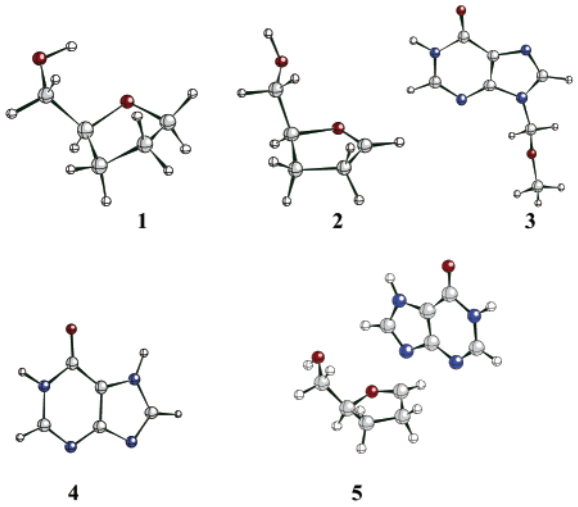

of TS, determined by Schramm and co-workers,[7,10] was used as an initial guess for TS geometry and refined further using ab initio calculations. The protocol used for TS parametrization is discussed in the following section.

Structure and Parameters for the Transition State. As there are no standard parameters describing the transition state for nucleoside hydrolysis in the CHARMM force field,[11] the parameters were obtained using an approach employed for the TS parametrization of diphtheria toxin-catalyzed NAD hydrolysis.[12,13] All of the ab initio calculations were done using the Gaussian 98 suite of programs.[14] Our methodology is similar to that previously used for NAD^+ hydrolysis. The complete TS structure was built upon on the experimentally determined partial TS structure.[7] The models used for the TS parametrization and structure refinement are presented in Chart 1.

Model **1** was used to describe the ribose moiety of the reactant inosine, and model **2** was used to represent the product ribooxocarbenium ion. Models **3** and **4** represent the hypoxanthine part of the reactant and the product, respectively. All of the models were first

(8) Miles, R. W.; Tyler, P. C.; Evan, G. B.; Furneaux, R. H.; Parkin, D. W.; Schramm, V. L. *Biochemistry* **1999**, *38*, 13147.
(9) Brooks, C. L., III; Karplus, M. *J. Mol. Biol.* **1989**, *208*, 159.
(10) Horenstein, B. A.; Schramm, V. L. *Biochemistry* **1993**, *32*, 9917.
(11) Brooks, B. R.; Bruccoleri, R. E.; Olafson, B. D.; States, D. J.; Swaminathan, S.; Karplus, M. *J. Comput. Chem.* **1983**, *4*, 187.
(12) Berti, P. J.; Schramm, V. L. *J. Am. Chem. Soc.* **1997**, *119*, 12069.
(13) Kahn, K.; Bruice, T. C. *J. Am. Chem. Soc.* **2001**, *123*, 11960.
(14) Frisch, M. J.; Trucks, G. W.; Schlegel, H. B.; Scuseria, G. E.; Robb, M. A.; Cheeseman, J. R.; Zakrzewski, V. G.; Montgomery, J. A.; Stratmann, R. E.; Burant, J. C.; Dapprich, S.; Millam, J. M.; Daniels, A. D.; Kudin, K. N.; Strain, M. C.; Farkas, O.; Tomasi, J.; Barone, V.; Cossi, M.; Cammi, R.; Mennucci, B.; Pomelli, C.; Adamo, C.; Clifford, S.; Ochterski, J.; Petersson, G. A.; Ayala, P. Y.; Cui, Q.; Morokuma, K.; Malick, D. K.; Rabuck, A. D.; Raghavachari, K.; Foresman, J. B.; Cioslowski, J.; Ortiz, J. V.; Stefanov, B. B.; Liu, G.; Liashenko, A.; Piskorz, P.; Komaromi, I.; Gomperts, R.; Martin, R. L.; Fox, D. J.; Keith, T.; Al-Laham, M. A.; Peng, C. Y.; Nanayakkara, A.; Gonzalez, C.; Challacombe, M.; Gill, P. M. W.; Johnson, B.; Chen, W.; Wong, M. W.; Andres, J. L.; Gonzalez, C.; Head-Gordon, M.; Replogle, E. S.; Pople, J. A. *Guassian 98*; Guassian, Inc.; Pittsburgh, PA, 1998.

optimized at the MP2/6-31+G(d,p) level. The bond length, bond angle, and torsion parameters for the transition state were estimated using the minimized structure of the models as the starting structure and the partial TS structure. The structure of the ribooxocarbenium TS was interpolated between models **1** and **2** on the basis of the knowledge of the published partial TS structure as derived from KIE[7] using the same methodology as described in refs 12 and 13. Similarly, the structure of the hypoxanthine ring was obtained by interpolating between the models **3** and **4**. The angle parameters for TS were obtained by performing an angle driver on model **5** for specific angles, such as O4′−C1′−N9 and H1′−C1′−N9. The parameters estimated from ab initio calculations were developed and tested using the CHARMM force field.

Atomic partial charges for the ribose part of substrate inosine in the presence of calcium cation were obtained from ab initio/RESP calculations as discussed in our previous paper.[6] The atomic charges for the transition state were obtained by interpolating the charge between the reactant and product models (see the Supporting Information).

MD Setup. The CHARMM27[11] topology and parameters were used for the protein, inosine, and TIP3P water model. Hydrogen atoms were added to the X-ray structure via the empirical energy placement protocol H-BUILD[15] in the CHARMM program. The protonation sites of histidine residues were based on the availability of H-bond donors or acceptors nearby. The His241 was protonated on both NE2 and ND1 sites for EH·S and EH·TS MD simulation and was neutral with proton on only ND1 in E·S and E·TS MD simulation. Aspartate, glutamate, arginine, and lysine residues were charged, and all of the tyrosine residues were neutral unless otherwise specified. Tyr229 carried a net negative charge in the MD simulation of both E·TS and EH·TS. The minimized structure of inosine and TS were docked in the enzyme active site on the basis of the knowledge of the binding interaction obtained by experimental studies and by overlaying with the previously published X-ray structure of the enzyme-transition state analogue inhibitor.[4] Eleven sodium ions were added to maintain the electroneutrality of the system.

The X-ray crystal structure places a nucleophilic water molecule Wat138 in position to occupy one of the coordination sites of the octacoordinated calcium ion. This water molecule (Wat138) is 3.3 Å from the ribosyl 1′-carbon of pAPIR bound to IU-NH in the X-ray crystal structure.[4] Preliminary simulation results showed that this water molecule does not exchange with waters from the water pool. A distance constraint was placed between the active site nucleophilic Wat138 and calcium ion using a force constant of 10 000 kcal/mol Å^2.[6] At the transition state, this water molecule is proposed to make a weak bond to the C1′-ribooxocarbenium ion with $R_{O\cdots C} = 3.0$ Å.[7] In the E·TS and EH·TS simulation, OH2 of Wat138 was constrained at a distance of 3.0 Å from C1′ without making any explicit bonds. A small force constant was placed on the oxygen (2′ and 3′ hydroxyl of ribose ring) to calcium distance ($R_{Ca\cdots O2} = 2.5$ Å, force constant = 10 kcal/mol Å^2; $R_{Ca\cdots O3} = 2.5$ Å, force constant = 10 kcal/mol Å^2) in each simulation.

A 42 Å water sphere was used to solvate the enzyme−ligand system. Any solvent molecule within 2.8 Å of a heavy atom of the enzyme or crystallographic water molecule was deleted. The system was separated into reaction zone and a reservoir region, and the reaction zone was further divided into the reaction region and the buffer region.[6] The system was partitioned using inosine and TS as the reference point in the E·S and E·TS MD simulations, respectively. The reaction region around an active site was the sphere of radius r of 40 Å, the buffer region was $40 < r < 42$ Å, and the reservoir region corresponded to $r > 42$ Å. Similar protocols for energy minimization and dynamics were used for all models. Before the start of the dynamics, the systems were energy minimized using the steepest descents (SD) method followed by adopted basis Newton−Raphson (ABNR) methods for 5000 steps. All atoms in the reservoir region were deleted after the minimization. All four models contained a total of ∼30 300 atoms after deletion of reservoir region atoms. The solvent molecules were equilibrated at 300 K for 3 ps, keeping the protein, ligand (S or TS), and the crystallographic water molecules fixed to allow favorable distribution of water molecules on the enzyme surface before the start of free dynamics. Another set of brief minimization was done before the start of dynamics using SD protocol. During the molecular dynamics simulation, the system was gradually heated by coupling to a heat bath of 150 K for 5 ps, 250 K for the next 15 ps, and 300 K for the rest of the simulation time using a frictional coefficient of 250 ps^{-1} on the heavy atoms of the enzyme. Heavy atoms of the protein in the buffer region were constrained using force constants calculated from their average Debye−Waller factors.[9] Bonds containing hydrogen were constrained using the SHAKE algorithm.[16] The nonbonded interactions were updated every 20 steps and were cut off at 12 Å by means of a force shifting function.

The MD simulations were carried out for 600 ps for H241A E·TS, 1000 ps for E·S and E·TS, and 1500 ps for both EH·S and EH·TS using a 1.0 fs time-step. The molecular dynamics results and its statistical analysis were carried out for the D-subunit after the first 200 ps for all four simulations. Covariance matrix was used to determine the extent of correlated motion between the α-carbons of the residues. MD trajectories were visualized using the program gOpenMol[17,18] to see the direction of anticorrelated motion between the desired residues. Also, a correlation plot was generated by plotting the distance of the desired residues from a reference point. For example, to observe the anticorrelated motion between the residues Asn168 and Tyr229, the distance trajectories of Asn168 (OD1)−Ala78 (CA) and Tyr229 (OH)−Ala78 (CA) were plotted against each other using Ala78 as a reference point.

Preliminary calculations were carried out on an SGI Indigo 2 workstation, and molecular dynamics simulations were performed on SGI Origin2000 at the UC Santa Barbara Supercomputing Center and CRAY T3E, University of Texas at Austin.

Results

Stability of Trajectory. The molecular dynamics simulations of solvated EH·S and EH·TS systems were carried out for 1.5 ns. The length of MD simulations of E·S and E·TS systems was 1 ns. As a measure of structural stability, root-mean-square deviations (rmsd) of the MD simulated structure from the starting structure were calculated on the basis of all of the backbone heavy atoms of EH·S and EH·TS systems (Figure 1). After an initial increase during the heating and equilibration period for the first 200 ps, a plateau is reached. The EH·TS simulation reached a plateau faster than the EH·S simulation. As shown in Figure 1, the average rmsd for the backbone (excluding hydrogen atoms) is 1.07 ± 0.159 Å for the EH·S simulation. The corresponding value for the EH·TS simulation is 1.01 ± 0.136 Å, respectively. After 200 ps, until the end of the simulation, the values fluctuate very little, indicating a stable and equilibrated protein structure. To reveal the most flexible regions of the protein structure, *B*-factors were calculated for the Cα atoms from the mean square fluctuation (msf) using eq 1[19,20]

$$B = \frac{8\pi^2}{3}(\text{msf}) \qquad (1)$$

(15) Brunger, A. T.; Karplus, M. *Proteins* **1988**, *4*, 148.
(16) Ryckaert, J. P.; Ciccotti, G.; Berendsen, H. J. C. *J. Comput. Phys.* **1977**, *23*, 327.
(17) Laaksonen, L. *J. Mol. Graphics* **1992**, *10*, 33.
(18) Bergman, D. L.; Laaksonen, L.; Laaksonen, A. *J. Mol. Graphics Modell.* **1997**, *15*, 301.

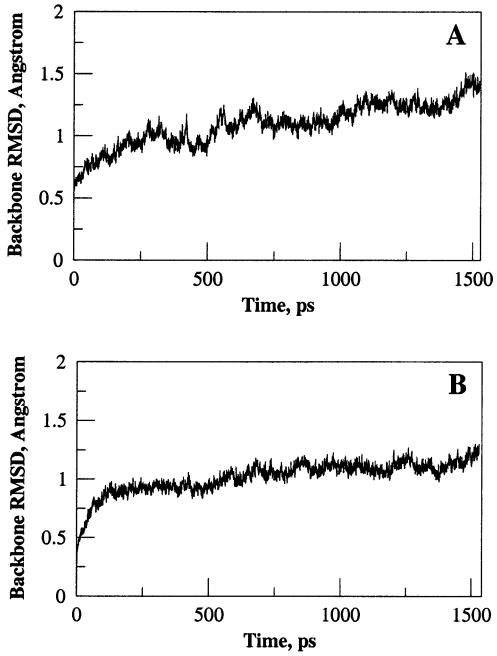

Figure 1. Time dependence of rms deviations of heavy atoms of EH·S (a) and EH·TS (b) during a 1.5 ns MD simulation.

The *B*-factors display major peaks in the regions of residues 80−90, 163−172, and 224−238. The calculated fluctuations are compared to values obtained from experimental *B*-factors (Figure S1, Supporting Information). Overall, the *B*-factors for all four MD simulations show very good consistency with the experimental *B*-factors from the X-ray crystal structure. The temperature of the system with respect to time remains steady within 300 ± 5 K over the course of the simulation.

Results from the MD Simulation of EH·S Using Native Enzyme. Enzymatic Interaction with the Ribose Ring of Substrate Inosine. Many contacts between the ribose ring of inosine and IU-NH active site residues were observed during the MD simulation of EH·S. The structural findings of enzyme−substrate contacts are more easily followed by referring to the structure shown in Figure 2A and Table 1. The average calcium to oxygen distances of the amino acids ligated to the octacoordinated calcium ion in the EH·S simulation are close to that provided by the X-ray crystal structure of inhibitor bound IU-NH: backbone carbonyl oxygen (O) of Thr126 (2.2 ± 0.06 Å), bidentate (OD1 and OD2) Asp15 (2.4 ± 0.1 Å, 2.2 ± 0.07 Å), OD2 of Asp242 (2.2 ± 0.06 Å), and OD2 of Asp10 (2.2 ± 0.06 Å). The above calcium−oxygen distances are stable throughout the dynamics.

Enzymatic contacts with the ribose ring include hydrogen bonds with all three hydroxyls. The hydrogen bonding distance between OE1 of Glu166 and O5′ of inosine is found to be short and stable during the MD simulation of EH·S. The short hydrogen bond between OD1 of Asp242 and hydrogen of O3′ of inosine ($R_{O\cdots O}$ = 2.5 ± 0.08 Å) prevailed during the dynamics. The ND2 of Asn168 remained within hydrogen bonding distance from the O3′ of the ribose ring ($R_{O\cdots O}$ = 2.9 ± 0.1 Å). The ribose ring O2′ of inosine is hydrogen bonded to OD2 of Asp14 ($R_{O\cdots O}$ = 2.6 ± 0.2 Å, Figure S2A, Supporting Information) throughout the MD simulation of EH·S. The ND2 of Asn39 is hydrogen bonded to O2′ ($R_{O\cdots O}$ = 3.3 ± 0.08 Å). The ribose ring adopts a C3′ exo conformation throughout the MD simulation. The OD1 of Asp10 remained within the distance of 2.9 ± 0.1 and 2.8 ± 0.1 Å from OD1 and OD2 of Asp15, respectively.

Enzymatic Contacts with the Hypoxanthine Ring (Leaving Group) of Substrate Inosine. The hypoxanthine binding pocket is lined with the polar residues His241, His82, Arg233, Tyr225, Tyr229 and nonpolar residues Phe167, Ile81. There are not many specific interactions between the hypoxanthine leaving group and active site residues as compared to those in the ribose part of inosine. The residues 224−238 in the aromatic leaving group pocket have high crystallographic *B*-factors. Figure 2B shows the active site hydrogen bonding pattern between inosine, Asp14, His241, Tyr225, and Tyr229.

The ND1 of His241 is hydrogen bonded to OD2 of Asp14 throughout the simulation ($R_{O\cdots O}$ = 2.9 ± 0.08 Å, Figure S3A, Supporting Information). The hydrogen on CE1 of His241 is found to make hydrogen bonds to OH of Tyr229 ($R_{O\cdots C}$ = 3.0 ± 0.08 Å, Figure 3A) and Tyr225 ($R_{O\cdots C}$ = 3.0 ± 0.20 Å, Figure 4A). The HH of Tyr225 is hydrogen bonded to the OH of Tyr229 (Figure 5A).

The network is completed by a hydrogen bond between the HH of Tyr229 to the N7 of inosine. Tyr229 is in one of the flexible loops in the leaving group pocket. On initiation of MD simulation, Tyr229 migrates closer to the N7 of hypoxanthine. This hydrogen bond is formed after the first 20 ps and is stable thereafter (Figure 6A). Arg233 is close to the hypoxanthine ring during the simulation, but no hydrogen bonding is observed. The NH1 of Arg233 is at a distance of 3.3 ± 0.44 Å from the O6 of the hypoxanthine ring, which is optimal for cation−π interaction.[21]

Results from the MD Simulation of EH·TS (Protonated His241) Using Native Enzyme. Enzymatic Interaction with the Ribose Ring of Transition State Inosine. All of the interactions present between the ribose moiety and the enzymatic residues during the MD simulation of EH·S prevailed during the EH·TS simulation. A hydrogen bond between the 2′-hydroxyl group of the ribooxocarbenium ion transition state and the OD1 of Asp14 is present for 98% of the observation time ($R_{H\cdots O} \leq$ 1.95 Å). The OD1 of Asp15 ($R_{O\cdots O}$ = 2.85 ± 0.11 Å) and OD2 of Asp242 ($R_{O\cdots O}$ = 2.87 ± 0.14 Å) contact O2′ of TS, but no hydrogen bonding is observed between them. The OD1 of Asp242 is hydrogen bonded to O3′ ($R_{O\cdots O}$ = 2.75 ± 0.09 Å). The O3′ is also hydrogen bonded to ND2 of Asn168 ($R_{O\cdots H}$ = 2.04 ± 0.16 Å). Apart from these interactions, OD1 of Asn168 is found to be closer to the O4′ of the TS as compared to EH·S ($R_{O\cdots O}$ = 4.4 ± 0.2 Å in EH·S, 3.8 ± 0.3 Å in EH·TS). The O4′ of the TS positions itself in between the oxygen of nucleophilic water (Wat138) and the O5′ of the ribooxocarbenium ion with an average angle between the OH2 of nucleophilic water (Wat138), O4′, and O5′ of the ribooxocarbenium ion of 135 ± 10°. The similar angle between the OH2 of nucleophilic water, N4′, and O5′ of pAPIR was found to be 163° in the crystal structure. The ND2 of Asn39 is hydrogen bonded to O2′ of TS ($R_{O\cdots O}$ = 3.2 ± 0.2 Å). The

(19) Brooks, C. L. I.; Karplus, M.; Pettitt, B. M. *Proteins: A Theoretical Perspective of Dynamics, Structure, and Thermodynamics*; Wiley-Interscience: New York, 1988; Vol. LXXXI.
(20) McCammon, J. A.; Harvey, S. *Dynamics of Proteins and Nucleic Acids*; Cambridge University Press: Cambridge, U.K., 1987.
(21) Burley, S. K.; Petsko, G. A. *Adv. Protein Chem.* **1988**, *39*, 125.

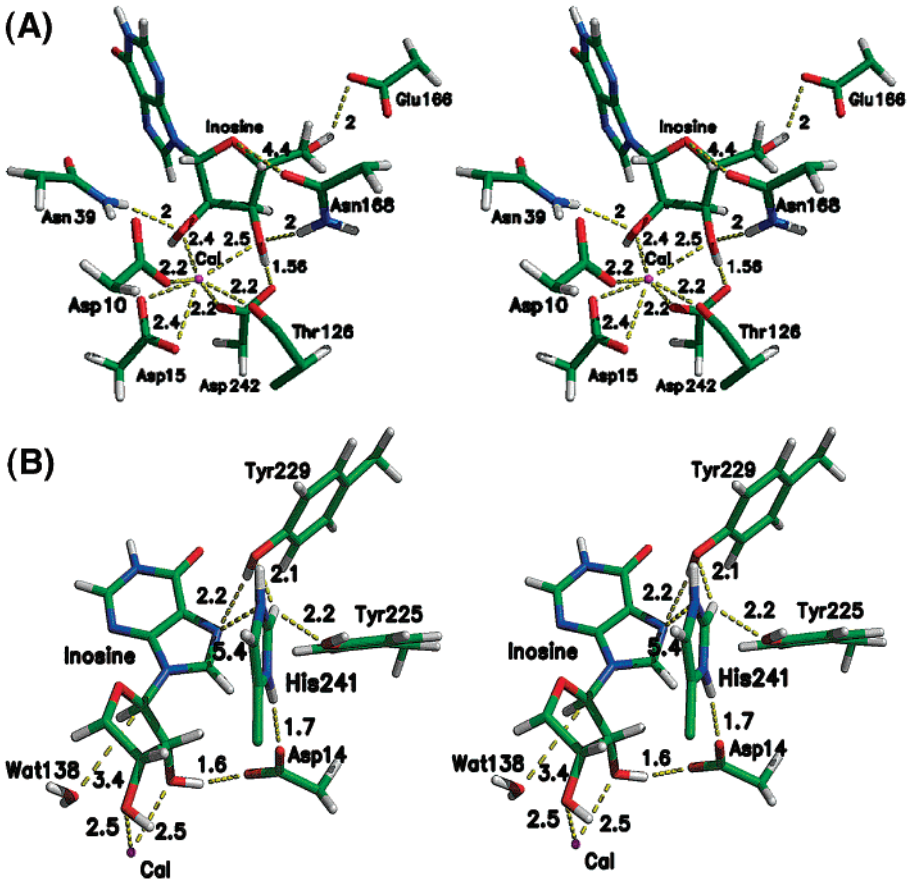

Figure 2. (A) Stereoimage of the active site residues of native EH·S interacting with the ribose part of inosine. Calcium is shown in magenta, hydrogen in white, carbon in green, oxygen in red, and nitrogen in blue. This represents the average structure from the MD simulation of EH·S. (B) Stereoimage of the active site residues of native EH·S showing the hydrogen bonding pattern between inosine, Asp14, Tyr225, Tyr229, and His241. Calcium is shown in magenta, hydrogen in white, carbon in green, oxygen in red, and nitrogen in blue. This represents the average structure from the MD simulation of EH·S.

Table 1. Comparison of Distances from X-ray (2MAS), EH·S, E·S, EH·TS, E·TS, E(H241A)·TS, and E·pAPIRH^{+} [6] [a]

	X-ray	EH·S	E·S	EH·TS	E·TS	E(H241A)·TS	E·pAPIRH^{+}
Asp14(OD1)−O2′	2.8	2.6 ± 0.2	2.6 ± 0.2	2.6 ± 0.1	2.6 ± 0.1	2.9 ± 0.2[d] A241 (N)	2.6 ± 0.2
Asp10(OD1)−Asp15(OD1)	3.1	2.9 ± 0.1	3.0 ± 0.1	2.9 ± 0.1	3.0 ± 0.1	3.0 ± 0.1	3.0 ± 0.1
Asp10(OD1)−Asp15(OD2)	3.1	2.8 ± 0.1	2.8 ± 0.1	2.7 ± 0.1	2.7 ± 0.1	2.7 ± 0.1	2.8 ± 0.1
Asp14(OD2)−His241(ND1)	3.6	2.9 ± 0.1	2.9 ± 0.2	2.7 ± 0.1	2.9 ± 0.2	2.8 ± 0.1[d] A241 (N)	2.7 ± 0.1
His241(CE1)−Tyr229 (OH)	2.9	3.0 ± 0.1	3.1 ± 0.1	3.8 ± 0.6	4.0 ± 0.5	8.4 ± 0.6[d] A241 (N)	3.5 ± 0.7
His241(CE1)−Tyr225(OH)	3.3	3.0 ± 0.2	3.1 ± 0.2	2.9 ± 0.1	3.0 ± 0.1	4.7 ± 0.3[d] A241 (N)	3.1 ± 0.2
Tyr225(OH)−Tyr229(OH)	3.9	3.6 ± 0.4	3.7 ± 0.4	2.7 ± 0.2	2.8 ± 0.2	5.8 ± 0.6	3.9 ± 0.5
His241(NE2)−N7	6.8[b]	5.2 ± 0.5	5.0 ± 0.4	5.4 ± 0.3	5.9 ± 0.4	7.7 ± 0.3	9.0 ± 1.4[b]
Tyr229(OH)−N7	4.5[b]	3.1 ± 0.4	2.9 ± 0.1	3.2 ± 0.3	3.1 ± 0.2	5.8 ± 0.8	7.3 ± 2.6[b]
Ile81(CD1)−C6	3.4[b]	8.7 ± 1.3	8.7 ± 0.9	4.3 ± 0.7	4.7 ± 0.5	6.7 ± 1.5	3.0 ± 0.2[b]
Asn168(OD1)−O4′	2.9[c]	4.4 ± 0.2	4.4 ± 0.2	3.8 ± 0.3	3.8 ± 0.3	4.1 ± 0.3	2.9 ± 0.2[c]
Asn168(ND2)−O3′	3.2	2.9 ± 0.1	2.9 ± 0.1	2.9 ± 0.1	2.9 ± 0.1	3.0 ± 0.1	2.9 ± 0.1
Asn39(ND2)−O2′	4.0	3.3 ± 0.3	3.2 ± 0.2	3.2 ± 0.2	3.2 ± 0.2	4.2 ± 0.8	3.1 ± 0.2
Arg233(NH1)−O6	4.1[b]	3.8 ± 0.1	2.9 ± 0.2	4.4 ± 1.1	4.0 ± 0.9	3.5 ± 0.8	5.0 ± 1.5[b]
His82(CE1)−N7	6.2[b]	5.4 ± 1.5	5.1 ± 1.0	6.0 ± 1.6	5.0 ± 0.5	3.8 ± 0.6	5.6 ± 0.6[b]

[a] All distances are given in angstroms. [b] Note that because N7, O6, and C6 are not present in the X-ray and E·pAPIRH^{+} structures, the corresponding distances are measured from pAPIR aniline ring nitrogen. [c] The distances corresponding to O4′ of ribose are measured from N4′ of inhibitor. [d] For E(H241A)·TS, the corresponding distances to His241 are measured from Ala241 (N).

OD1 of Asp10 remained within the distance of 2.9 ± 0.1 and 2.7 ± 0.1 Å from the OD1 and OD2 of Asp15, respectively.

Enzymatic Interaction with the Hypoxanthine Ring of the Transition State Inosine. As in EH·S, the hypoxanthine leaving group has less contact with the surrounding residues as compared to the ribooxocarbenium part of TS.

A hydrogen bonding network (Figure 7) between inosineO2′-Asp14-His241-Tyr225- Tyr229-inosineN7 is found to be present during the MD simulation of E·TS. The distance time series for these interactions are shown in Figures 3−6 (also examine Figures S2−4, Supporting Information). Unlike MD simulation of EH·S, the hydrogen bonds from His241 to Tyr229 and

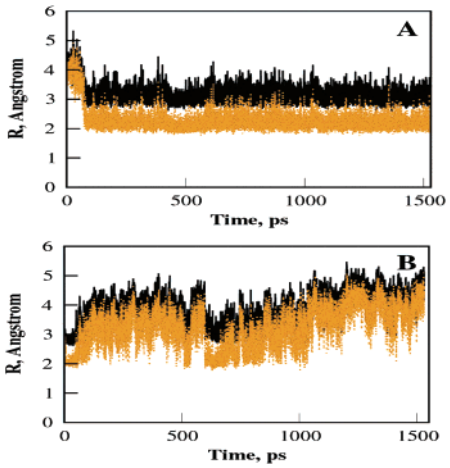

Figure 3. Formation and breaking of the hydrogen bond between hydrogen on CE1 of His241 and OH of Tyr229 in MD simulations of EH·S (A) and EH·TS (B). The solid black line shows the heavy atom distance, $R_{O\cdots O}$, and the orange dotted line shows the distance between the oxygen and hydrogen atom, $R_{O\cdots H}$.

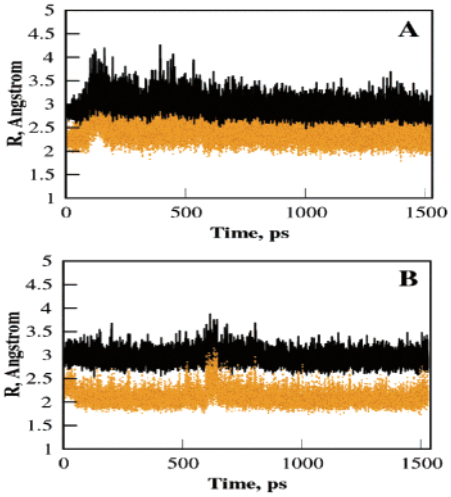

Figure 4. Formation and breaking of the hydrogen bond between hydrogen on CE1 of His241 and OH of Tyr225 in MD simulations of EH·S (A) and EH·TS (B). The solid black line shows the heavy atom distance, $R_{O\cdots O}$, and the orange dotted line shows the distance between the oxygen and hydrogen atom, $R_{O\cdots H}$.

Tyr225 are not bifurcated. The hydrogen on CE1 of His241 is hydrogen bonded for 2% of the time to OH of Tyr229 and 33% of the time to Tyr225 ($R_{O\cdots H} \leq 2$ Å). The HH of Tyr225 is hydrogen bonded to Tyr229 ($R_{O\cdots O} = 2.7 \pm 0.2$ Å). The hypoxanthine ring is stabilized by hydrophobic contact with Ile81 ($R_{C6\cdots CD1} = 4.7 \pm 0.5$ Å), which is not present in the ground state ($R_{C6\cdots CD1} = 8.7 \pm 1.3$ Å for ground state). The NH1 of Arg233 is at a distance of 4.4 ± 1.1 Å from the O6 of the hypoxanthine ring.

Results from the MD Simulation of E·S and E·TS (Neutral His241 Using Native Enzyme). Nanosecond MD simulations of E·S and E·TS produced stable trajectories after the initial heating and equilibration phase. All of the observed interactions between the ribose moiety and the enzymatic residues in the MD simulation of EH·S and EH·TS prevailed during the E·S and E·TS simulations, respectively. The hydrogen bonds between the ND1 of His241 and OD2 of Asp14 ($R_{O\cdots O} = 2.9 \pm 0.2$ Å), CE1 of His241 and OH of Tyr225 ($R_{C\cdots O} = 3.1 \pm$

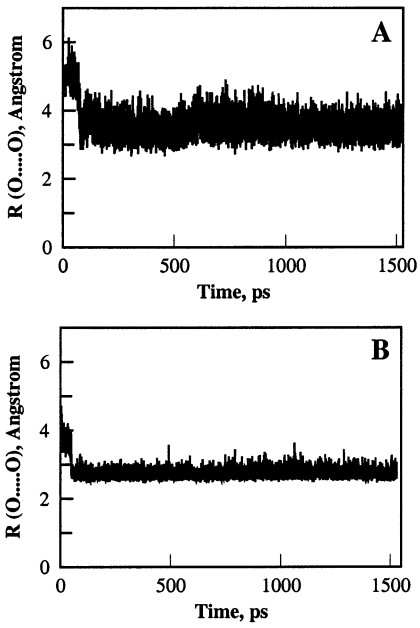

Figure 5. Relocation of Tyr229 during MD simulation. Hydrogen bonding interaction between the OH of Tyr225 and Tyr229 in MD simulations of EH·S (A) and EH·TS (B).

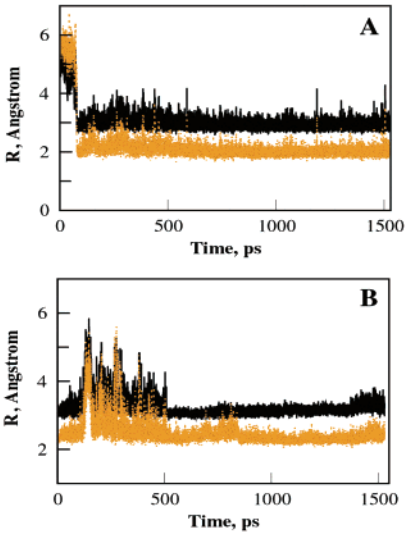

Figure 6. (A) Motion of Tyr229 during MD simulation. Hydrogen bonding interaction between HH of Tyr229 and N7 of inosine in MD simulation of EH·S. (B) Hydrogen bonding interaction between OH of tyrosinate anion Tyr229 and H7 of ribooxocarbenium ion TS from MD simulation of EH·TS. The solid black line shows the heavy atom distance, $R_{O\cdots O}$, and the orange dotted line shows the distance between the oxygen and the hydrogen, $R_{O\cdots H}$.

0.2 Å), and OH of Tyr229 and inosine N7 ($R_{O\cdots O} = 3.1 \pm 0.1$ Å) are essentially the same as those observed with the EH·S. No hydrogen bonds formed or broke during the E·TS simulation with neutral His241. Thus, no major structural changes occur in the active site on protonation of His241.

Results from the MD Simulation of E·TS Using His241Ala Mutant Enzyme. A short-term MD simulation on E·TS (600 ps) is performed using the His241Ala mutant enzyme to study the effects of the mutation. The average structure of the active site from the mutant enzyme simulation is shown in Figure 8.

During the simulation, O2′ of ribooxocarbenium ion is hydrogen bonded to OD1 of Asp14 ($R_{O\cdots O} = 2.9 \pm 0.2$ Å,

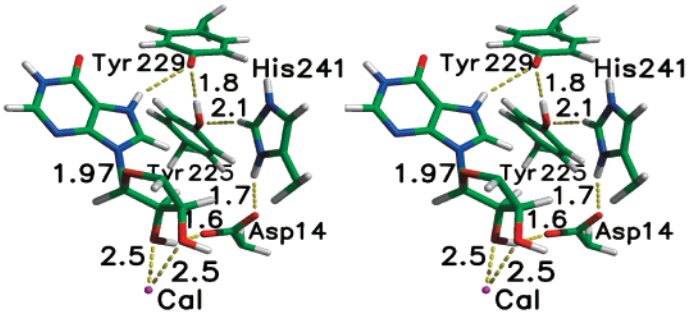

Figure 7. Average structure showing the hydrogen bonding network between O2′-Asp14-His241-Tyr225-Tyr229-N7 during MD simulation of EH·TS. The hydrogen bonds are shown by the dotted yellow line. The average hydrogen bond distances ($R_{O\cdots H}$) from MD simulation are shown in the figure.

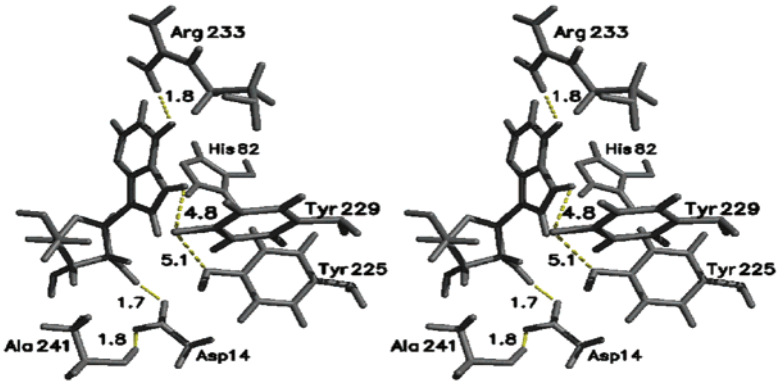

Figure 8. Average structure from the MD simulation of EH·TS using H241A mutant enzyme showing various distances averaged over simulation time. Mutation of His241 to Ala results in the loss of hydrogen bond between the residue 241 and 229. This allows Tyr229 to move away from inosineN7. Arg233 is hydrogen bonded to the O6 of inosine.

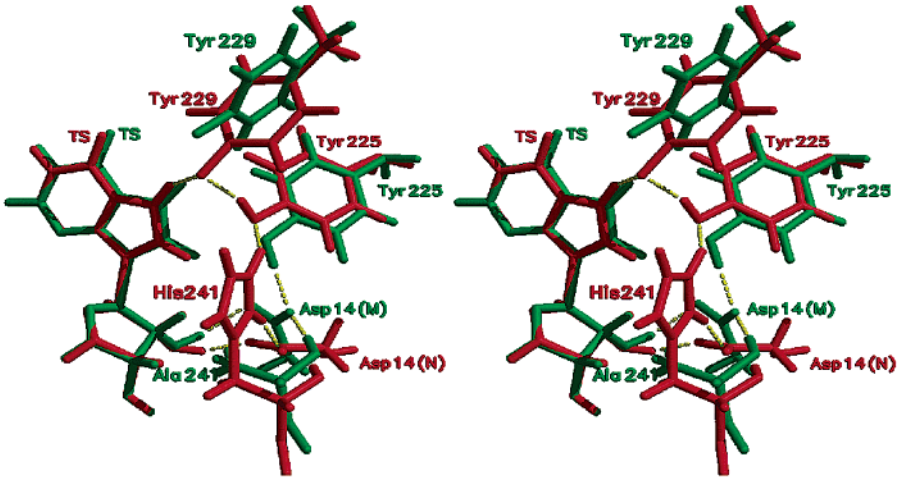

Figure 9. Superposition of the average structures from MD simulations of the native and H241A mutant EH·TS. The native enzyme is shown in red, and the mutant is shown in green. The figure shows the loss of crucial hydrogen bonds in the mutant enzyme.

Figure S4, Supporting Information). The hydrogen bond between the ND1 of His241 and OD2 of Asp14, which prevailed during the native E·TS simulation, is replaced by a hydrogen bond between the backbone amide (H) of Ala241 and OD2 of Asp14 ($R_{O\cdots N} = 2.8 \pm 0.1$ Å). The average structure from H241A mutant E·TS is superimposed on the average structure generated by MD simulation on the native EH·TS in Figure 9. No hydrogen bonds are observed between Tyr225, Tyr229, and TS (Figure S4, Supporting Information). The mutant enzyme loses the hydrophobic contact with the aromatic ring when residue Ile81 drifts away ($R_{O\cdots O} = 6.7 \pm 1.5$ Å). However, a hydrogen bond between O6 of TS and HH12 of Arg233 is observed ($R_{O\cdots N} = 3.5 \pm 0.8$ Å).

Atomic Motions During the MD Simulation of E·S and E·TS. Analysis of atomic correlation motion revealed that several residues moved in a concerted manner. Correlation plots generated from the MD simulation of EH·S, E·S, EH·TS, and E·TS are shown in Figure 10 A. Almost all of the residues that are positively correlated during EH·S MD showed a similar correlation pattern during EH·TS MD simulation. The negative correlated motion is predominant in EH·S and E·S as compared to EH·TS and E·TS. The residues 216−236 and 157−172 exhibit substantial anticorrelated motion toward each other in EH·S, but not in EH·TS. These residues are part of the active site region. The residues Asn168 and Tyr229 show negative correlation for 37% of the time in EH·S and 29% of the time

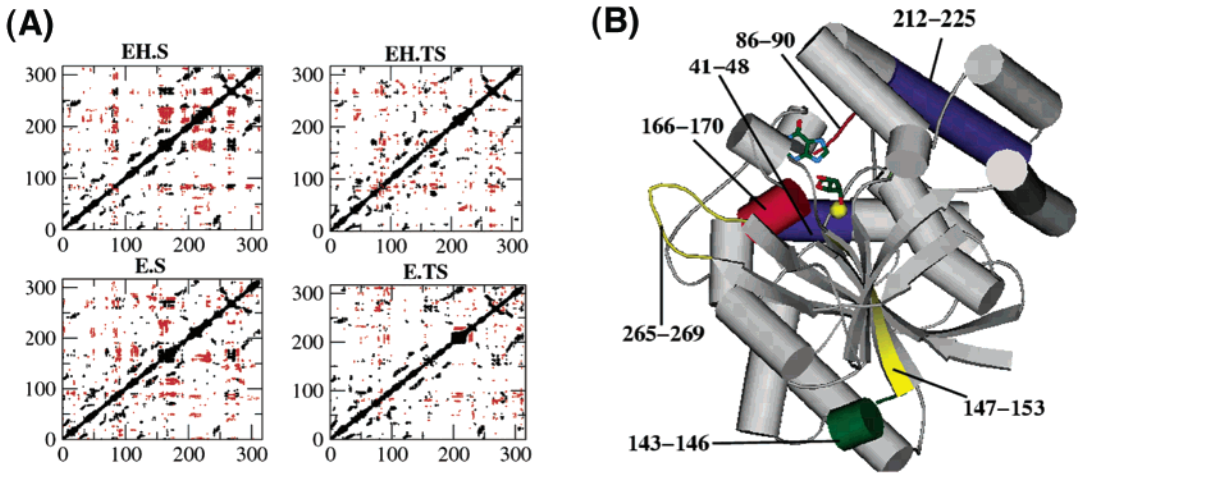

Figure 10. (A) Negative and positive correlated motions observed during the production phase of MD simulation of EH·S, E·S, EH·TS, and E·TS. The positive and negative correlations (25%) are shown in black and red, respectively. The negative correlation pattern is predominant in EH·S and E·S as compared to that in EH·TS and E·TS. (B) Positions of some of the residues displaying negative correlated motion (25%) with each other are marked with a similar color. The figure shows the position of the residues with respect to the active site from EH·TS MD simulation. For example, residues 166−170 and 86−90 show anticorrelated motion and are shown in red. Calcium is shown as a yellow ball, and a green stick model represents the transition state. Plot generated with program MOLSCRIPT.[22]

in E·S. A plot can be generated to show the extent of anticorrelation between the two residues using Ala78 as the reference point (Figure S5, Supporting Information).

The loop containing the residues 156−159 and 164 displayed a strong positive correlation (~40%) with the loop containing residues 266−273. The anticorrelation pattern changed significantly while going from the EH·S to EH·TS MD simulation. In the MD simulation of EH·TS, the following anticorrelated motions are observed (Figure 10B): the helices containing residues 166−170 and 212−225; helix containing the residues 41−48 with the loop residues 86−90; and the β-sheet residues 147−153 with the loop residues 265−269.

Discussion

The catalytic rate enhancement by purine *N*-ribohydrolases is estimated to be 6×10^{12} relative to the uncatalyzed reaction.[23] Despite the extensive kinetic and structural work, there are some gaps in understanding the mechanism and role of different active site residues of purine nucleoside hydrolases, especially the role of residues in the leaving group pocket. Using *in silico* techniques, we have investigated enzyme bound to natural substrate and TS using TIP3P water as a solvent to hydrate the system.

MD simulations were carried out on the following systems: enzyme·substrate with protonated His241 (EH·S), enzyme·substrate with neutral His241 (E·S), enzyme·transition state with protonated His241 (EH·TS), enzyme·transition state with neutral His241 (E·TS), and the His241Ala mutant E(H241A)·TS systems. The His241 is positively charged with protons on the NE2 and ND1 site in EH, whereas it is neutral with a proton on the ND1 site in E. All five systems produced stable trajectories. Lower *B*-factors are observed for the residues surrounding the sugar moiety as compared to those in the leaving group pocket. This justifies that the leaving group pocket of IU-NH is flexible and can take both inosine and uridine as a substrate even though the base sizes are different.

Chart 2. Putative Residues for Catalysis[a]

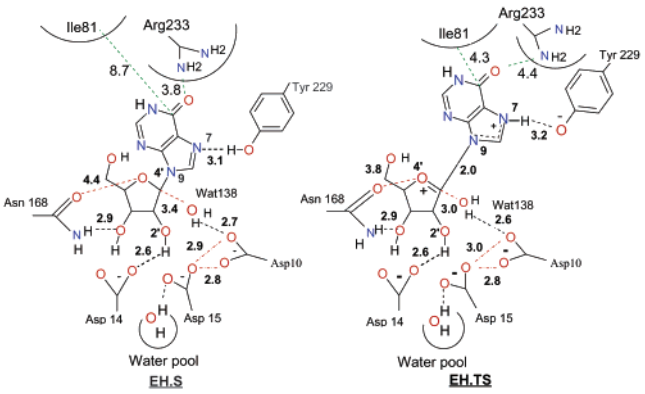

[a] Hydrogen bonds shown by black line, electrostatic interaction shown by red dotted line, and hydrophobic interaction shown by green dotted line. Distances are shown for heavy atoms in angstroms. Access of Asp15 to water pool is also shown.

The distances that significantly differ between the structures generated from MD simulations and X-ray can be viewed in Table 1. It is known that the primary sequence, Asp14, Tyr225, Tyr229, and His241, is conserved in IU-NH from both *Crithidia fasciculata* and *Leishmania major*. The available crystal structure (2MAS) reveals close contact between the ribose part and the surroundings. The MD simulations with EH·S and EH·TS support this fact. All three ribose hydroxyls are hydrogen bonded to the active site carboxylates (Asp14, Asp242, and Glu166). The short hydrogen bond between the O2′ of ribose and OD1 of Asp14 might play a role in nucleoside hydrolase catalysis (vide infra). Apart from hydrogen bonds to the negatively charged carboxylates, neutral residues such as Asn39 (ND2) and Asn168 (ND2) are also hydrogen bonded to O2′ and O3′, respectively, in the structures generated from the MD simulations of EH·S and EH·TS.

The active site residues that might be important for catalysis are shown in Chart 2. The OD1 of residue Asn168 is at a distance of 4.4 ± 0.2 Å from the O4′ of inosine in the structure generated by MD simulation of EH·S. This distance shortens by about 1 Å in the EH·TS structure, bringing OD1 of Asn168

(22) Kraulis, P. J. *J. Appl. Crystallogr.* **1991**, *24*, 945.
(23) De Wolf, W. E. J.; Fullin, F. A.; Schramm, V. L. *J. Biol. Chem.* **1979**, *254*, 10868.

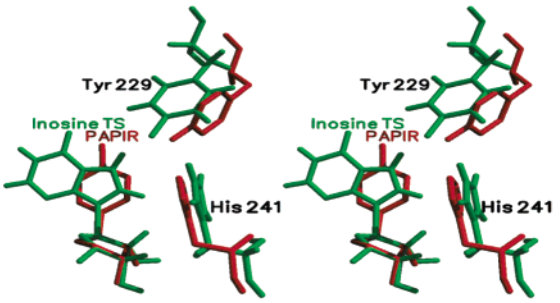

Figure 11. Stereoimage comparing the position of His241-Tyr229-ligand from X-ray (2MAS) and average structure from EH·TS MD simulation. Note that Tyr229 in X-ray is closer to pAPIR as compared to His241.

closer to O4′ of ribooxocarbenium ion TS. In our previous MD simulation,[6] Asn168 was proposed to stabilize the TS analogue inhibitor pAPIR through a hydrogen bond from N4′ to OD1 of Asn168 (Table 1). This can also be a crucial interaction for stabilization of the ribooxocarbenium ion TS. Another factor that could stabilize the ribooxocarbenium ion TS is the "sandwich" geometry of O4′ between O5′ ($R_{O\cdots O} = 3.0 \pm 0.09$ Å) and OH2 of the nucleophilic water (Wat138) molecule ($R_{O\cdots O} = 3.2 \pm 0.09$ Å) with the average angle of $135 \pm 10°$ during the MD simulations of EH·TS and E·TS. The hydrophobic interactions with Ile81 could also stabilize the TS over ground state. However, the residue Arg233, which stabilized the ground state by a cation$-\pi$ interaction, moves away from the π-ring of TS by about 1 Å.

For the catalytic activity of the enzyme, a group with a pK_{app} of 9.1 must be protonated, and another group with a pK_{app} of 7.1 must be unprotonated.[5] On the basis of its location in the active site, His241 was proposed to play a role in protonation of the leaving group at N7.[2,5] However, during the MD simulation of EH·S, E·S, EH·TS, and E·TS, His241 was never found to interact with the N7 of hypoxanthine. Instead, Tyr229 migrated within the first few picoseconds to make a stable hydrogen bond to N7 thereafter (Chart 2 and Figure 6). In the published X-ray crystal structure (2MAS), the residue Tyr229 is closer to the base (aniline ring in case of pAPIR, 2MAS) as compared to His241 by about 2 Å. The superposition of the X-ray (2MAS) structure and the average structure from the MD simulation of EH·TS shows good agreement between both (Figure 11). In a previous simulation, we showed Tyr229 to interact with the TS analogue, pAPIR, for the first 300 ps, whereas no interaction with His241 was observed for pAPIR.[6] The pH dependence of kinetics supports our simulation results. Thus, a pK_{app} of 9.1 is most appropriate for the tyrosine instead of the histidine residue. However, His241 does play a very crucial role in catalysis by assistance in the organization of the residues in the leaving group pocket (Figure 9). The findings from all four MD simulations support Tyr229 as the protonating agent. Protonation of His241 has essentially no effect on the structures of EH·S versus E·S and EH·TS versus E·TS (Chart 3).

A further understanding of the role of His241 was obtained from the MD simulation of E·TS using the His241Ala mutant enzyme (Figures 8, 9, and Figure S4, Supporting Information). The experimentally observed 2100-fold drop[2] in k_{cat} due to mutation can be attributed to the fact that active site organization by His241 through hydrogen bonding to Tyr225, Tyr229, and Asp14 is disrupted on this mutation. It's evident from Figure 9

Chart 3

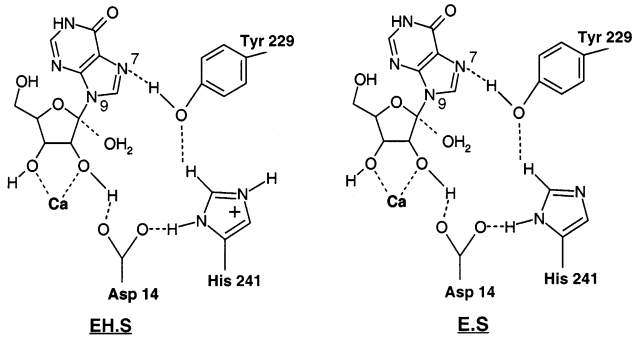

that His241 is the residue that is responsible for holding together the catalytically important machinery for protonation of the leaving group.

Originally, it was proposed that the residual activity (10^{-3}) of the His241Ala mutant could occur from an alternate proton donor.[2] Indeed we see during the MD simulation that there are a few enzymatic residues, which might act as possible proton donors in the His241Ala mutant (Figure 8). Hydrogen bonding of the NH1 of Arg233 to the O6 of TS exists for 48% of the time during the MD simulation of the His241Ala mutant. Such a hydrogen bond was not present in the MD simulations of native EH·S and EH·TS. A possible candidate for proton donor can be His82, which is at close vicinity (~3.8 Å) to the hypoxanthine ring.

The group which appears with a pK_{app} of 7.1 was originally proposed to be one of the active site carboxylates with an elevated pK value.[5] On the basis of the function and position during the MD simulations, Asp10 or Asp15 can be possible candidates. An elevated pK_a value for these carboxylates is justified by considering the distance from each other during the MD simulations. The OD1 of Asp10 has close contact with the OD1 and OD2 of Asp15 (Chart 2). This could possibly lead to a higher pK_{app} of Asp10 or Asp15. Asp10 has been proposed to act as a general base, abstracting a proton from the nucleophilic water molecule, Wat138.[4] Negatively charged Asp10 will facilitate the deprotonation of water effectively rather than the hydrogen bonded aspartate. Thus, deprotonation of Asp10 or Asp15 will trigger the catalysis. Asp15 is hydrogen bonded to the bulk solvent (Chart 2), which can act as a channel to transfer the proton from Wat138 → Asp10 → Asp15 → water pool. Aspartates with elevated pK_a have been reported earlier for enzymes such as ketosteroid isomerase[24] and human thioredoxin.[25]

During MD simulations of EH·S, E·S, EH·TS, and E·TS, as well as a previous MD simulation study of E·pAPIR,[6] it was found that the short hydrogen bonds between the OD2 of Asp14 and ribose O2′ as well as OD1 of Asp14 and ND1 of His241 were persistent throughout the simulations (Chart 2 and Figures S2, S3, Supporting Information). The hydrolysis of NAD^+ in water is facilitated by specific base catalysis.[26] At pH values above 11, the ribose 2′-OH is ionized, and the rate constant for hydrolysis is increased by 10 000-fold.[26] In a recent computational study of the diphtheria toxin (catalytic subunit)-catalyzed

(24) Thornburg, L. D.; Hénot, F.; Bash, D. P.; Hawkinson, D. C.; Bartel, S. D.; Pollack, R. M. *Biochemistry* **1998**, *37*, 10499
(25) Andersen, J. F.; Sanders, D. A. R.; Gasdaska, J. R.; Weichsel, A.; Powis, G.; Montfort, W. R. *Biochemistry* **1997**, *36*, 13979.
(26) Johnson, R. W.; Marschner, T. M.; Oppenheimer, N. J. *J. Am. Chem. Soc.* **1988**, *110*, 2257.

NAD^+ hydrolysis, an active site carboxylate (Glu148) was found to be hydrogen bonded to the ribose O2′ for 17% of the time in the ground state.[13] This hydrogen bonding to Glu148 does not contribute to the 6000-fold rate enhancement of NAD^+ hydrolysis by diphtheria toxin. Thus, Glu148 can be mutated to Asp or Gln with little effect on k_{cat} for the NAD^+ hydrolysis by diphtheria toxin.[27] It is hard to conceive that the hydrogen bond to the carboxylate of glutamate is of no importance in the hydrolysis of NAD^+ by diphtheria toxin. With the *Cf* IU-NH system, the rate enhancement of enzyme-catalyzed over the uncatalyzed reaction is of the order 10^{12}, and the hydrogen bond between ribose O2′ and OD1 of Asp14 is present for about 96% of the time during MD simulation of EH·TS. The partial negative charge developed due to hydrogen bonding to ribose O2′ could stabilize the formation of an oxocarbenium ion through inductive effects. Schramm and co-workers have observed an unusually large 2′-^{3}H kinetic isotope effect (1.161) for C2′ in the transition state.[7] On the basis of these KIE data, it was suggested that the hydrogen bond to ribose O2′ increases the electron density of the C2′−H2′ bond, contributing to the large vibrational freedom of H2′.[7] It is also observed that 2′-deoxynucleosides are poor substrates of nucleoside hydrolase.[28] Mutation of Asp14 to Gln would shed light on the importance of Asp14.

The MD simulations of the ground state and transition state produced interesting correlation patterns (Figure 10A,B). The negative correlation patterns exhibited by EH·S and E·S are significantly different as compared to those generated from EH·TS and E·TS, respectively. The anticorrelated motion is predominant between the active site residues 216−236 and 157−172 in the ground state. The former residues are part of the leaving group pocket, and the latter are part of the ribose binding region. The protonation of His241 provides greater correlation in MD simulation of enzyme complexes of S and TS. The correlation motion is predominant in the enzyme complexed with S regardless of the protonation state of His241. The residues Asn168 and Tyr229 show anticorrelated motion with each other for 37% of the time in EH·S and 29% of the time in E·S. Asn168 and Tyr229 are two crucial residues for catalysis. The former is associated with the stabilization of the positively charged ribooxocarbenium ion TS, and the latter is responsible for protonation of the leaving group at N7. The ground-state conformers where the OH of Tyr229 comes closer to N7 of inosine and the OD1 of Asn168 migrates closer to O4′ of the ribose ring can be looked upon as "NAC" or near attack conformers that will facilitate the formation of TS.

A good consistency in geometry between the X-ray and MD simulated structures was observed for the residues interacting with the ribose moiety. The present studies suggest analysis of the catalytic properties of mutant enzymes where Tyr229 and Tyr225 have been replaced. Kinetic studies using the mutants of Asp14 might also provide interesting results.

Acknowledgment. The National Science Foundation Grant MCB-9727937 supported this research. The authors would like to thank Prof. Vern Schramm for providing the transition state structures and suggestions. We are grateful to Dr. Kalju Kahn for technical advice and helpful discussions. The authors acknowledge computer facilities provided by SGI Origin2000 at the UC Santa Barbara Supercomputing Center and CRAY T3E, University of Texas at Austin.

Supporting Information Available: Charges and parameters for TS, Figures S1 (positional fluctuations for the α-carbons), S2 (distance trajectories showing the distance between the OD1 of Asp14 and O2′), S3 (distance between the HE1 of His241 and OD2 of Asp14), S4 (results from MD simulation of H241A mutant E·TS), and S5 (anticorrelated motion between the residues Asn168 and Tyr229) (PDF). This material is available free of charge via the Internet at http://pubs.acs.org.

JA021088E

(27) Wilson, B. A.; Reich, K. A.; Weinstein, B. R.; Collier, R. J. *Biochemistry* **1990**, *29*, 8643.
(28) Parkin, D. W.; Horenstein, B. A.; Abdulah, D. R.; Estupiñán, B.; Schramm, V. L. *J. Biol. Chem.* **1991**, *266*, 20658.